Int. J. Appl. Comput. Math (2019) 5:24
https://doi.org/10.1007/s40819-019-0608-0

ORIGINAL PAPER

Numerical Solutions of Dissipative Natural Convective Flow from a Vertical Cone with Heat Absorption, Generation, MHD and Radiated Surface Heat Flux

R. M. Kannan[1] · Bapuji Pullepu[1] · Sabir Ali Shehzad[2]

Published online: 1 February 2019

Abstract
The laminar natural convective hydromagnetic viscous fluid flow induced by a cone under aspect of radiated heat flux with thermal radiation, heat absorption and generation is addressed here. The basic equations of conservation of momentum, mass and energy are utilized for the modeling of physical problem. The consequential expressions are worked out by using Crank–Nicholson approach. The implementation of this method leads to conversion of non-dimensional expressions into system of tri-diagonal expressions. The obtain numerical data is visualized for momentum, local-average shear stresses, rate of heat transportation and temperature for various constraints *Pr*, Δ, *M*, ε and *Rd* with the help of graphical sketches. It is reported that the temperature of liquid is boost up with an enhancement in heat generation constraint. The larger Prandtl number corresponds to weaker temperature profiles. The average shear stress coefficient increase for higher radiation constraints and Prandtl number.

Keywords Finite difference method · MHD · Thermal radiation · Viscous dissipation · Vertical cone

List of Symbols

$F_0''(0)$	Shear-stress co-efficient in Ref: [13]
Gr_L	Grashof number
g	Rate of change of velocity due to gravity
k	Thermal conductivity
k^*	Mean sink co-efficient
L	Reference span
M	Magnetic constraint
Nu_x	Local Nusselt number
$\underline{Nu}_X$	Dimensionless Local Nusselt numeral
$\overline{Nu}$	Dimensionless average Nusselt numeral

✉ Sabir Ali Shehzad
ali_qau70@yahoo.com

[1] Department of Mathematics, SRMIST, Kattankulathur, Tamil Nadu 603 203, India

[2] Department of Mathematics, COMSATS University Islamabad, Sahiwal 57000, Pakistan

Pr	Prandtl number
q_w	Uniform wall heat flux per unit area
R	Non-dimensional local radius of the cone
r	Local radius of the cone
T'	Temperature
T	Non-dimensional temperature
t'	Time
t	Non-dimensional time
U	Non-dimensional velocity in X-direction
u	Velocity component in x-direction
V	Non-dimensional velocity in Y-direction
v	Rate component in y-direction
X	Non-dimensional spatial co-ordinate
x	Spatial coefficient along cone generator
Y	Non-dimensional spatial coefficient along the normal to the cone generator
y	Spatial coefficient along the normal to the cone generator

Greek Symbols

α	Thermal diffusivity
β	Volumetric thermal expansion
σ	Electrical conductivity
σ^*	Stefan–Boltzmann constant
Δ	Non-dimensional heat source/sink constraint
Δt	Non-dimensional time step
ΔX	Non-dimensional finite difference grid size in X-direction
ΔY	Non-dimensional finite difference grid size in Y-direction
ε	Viscous dissipation parameter
ϕ	Semi vertical angle of the cone
μ	Dynamic viscosity
γ	Kinematic viscosity
ρ	Density
τ_x	Non-dimensional local skin friction
τ_X	Non-dimensional local skin friction
$\bar{\tau}$	Non-dimensional average skin friction

Subscripts

w	Condition on the wall
∞	Free stream condition

Introduction

In this paper the main discussion encountered the impacts of natural convection with viscous incompressible fluid and its rate of flow of particles across a given surface. It has been detected that significant dissipation due to viscous liquids can arise in natural convection in different equipment due to huge quantity of decelerations or which function of huge speed. The application includes cooler or chilling the nucleus or kernel of atomic reactor, The transfer of heat through a liquid or gas caused by molecular motion in natural

medium consisting of laminar layer of slower stream of fluid past a surface on an electrically accomplishing liquid in the occurrence of a magnetic field. This aspect were considered by several investigators for the reason that it has industrial and technological uses namely bulging of plastics in the making of a synthetic silk like fabric and thermoplastic polyamide, refining of dark oil consisting mainly of hydrocarbons, processing of magnetic materials, producing a brittle transparent solid with irregular atomic structure, paper industry called radiative hydrodynamics etc. The area of MHD pump into various manufacturing and ecological methods, e.g., heating and chilling chambers and dehydration from huge open water reservoirs, planetary flows and energy from the sun that is converted into thermal or electrical energy technology. The gluey debauchery on free convection has been considered by Gebhart [1]. Alamgir [2] analyzed an integral technique to evaluate the whole heat transport from upright cones in laminar usual convective flow. Raptis [3] discussed unsteady 2-dimensional free convection flow of a voltically conducting viscous and non-compressible fluid along an infinite vertical plate embedded in a permeable medium. Presently numerical studies on laminar natural convective flow of axi-symmetric fluid have established large interest particularly in case of homogeneous and variable surface heat flux. Similarly solution for the laminar natural convection from a right circular cone with prescribe homogeneous thermal flux circumstances for different value of Prandtl number (i.e. $Pr = 0.72$, 1.0, 2.0, 4.0, 6.0, 8.0, 10, 100) and notations for both walls and wall temperature distributions at $Pr \to \infty$ be described by Lin [4]. Chen et al. [5] acquired numeral classification for mixed convective thermally scattered flow through a fluid–saturated absorptive medium to review the complete mixed convection system from the unpolluted forced convection limit to the pure natural convection limit. Their analysis was that non-darcian and heat distribution effect have a predominant effect happening rate profiles, thermal and heat dispersion velocities from the upright surface.

Vajravelu and Nayfeh [6] presented hydro magnetic convection from a cone and wedge with alteration surface thermal and interior heat source/sink. The effects of temperature boundary layer convection flow with optimism and suction/injection is discussed by Hossain and Paul [7]. Bapuji et al. [8] discussed unsteady natural convective phenomenon from an upright cone with isothermal surface heat flux. Bapuji and Chamkha [9] extended the earlier job below the condition of variable thermal flux with MHD effects. Kumari and Nath [10] focused the non-Darcy free convection current of Newtonian solution on an upright cone encapsulated in a saturated material with competency law alteration of the wall thermal/concentration and suction/injection. Sunitha et al. [11] has analyzed the transient radioactive hydro magnetic natural transmission flow past an abruptly on track upright sheet homogeneous heat and concretion flux.

Zueco [12] accounted by NSM to learn the outcomes of adhesive dissipation and induction heat on transient MHD natural convection movement over an upright permeable plate. The mixed convection over an unstable broadening porous surface has been demonstrated by Khan et al. [14, 15]. Hossain and Paul [13] considering the variable solution for the natural transmission from an upright permeable cone with non-affinity surface temperature. Mohammed et al. [16] invented that MHD natural transmission of thermal and bulk shift boundary surface flow of viscous, non-compressible and visibly thick liquid throughout a permeable medium along a spontaneously moving heat vertical plate in the existence of uniform chemical react of first sort and temperature dependent hot exchanger. For more discussion on magneto convective flows, the readers can consult the studies [17–22].

Cookey et al. [23] discussed the viscous dissipation and emission on unstable MHD natural convection flow past an enormously heated plate in a permeable material with moment related suction. Chen [24] explored thermal and bulk transport via free convection

of power-law fluid past an upright uniform cone surface. The cone surface is sustained at non-varying thermal and non-varying species attentiveness. The natural convective flow of a viscous non-compressible fluid through an enormous upright swinging plate of homogeneous thermal flux in the being there of induction heat was analyzed by Chandrakala [25]. Seth et al. [26] evaluated the unsteady hydro-magnetic free convection flow with thermal and bulk transmission of an electrically conducting, adhesive, non-compressible, chemically reacting and heat consuming aqueous solution past in fastened moving upright plate with heightened temperature and heightened surface absorption through a spongy medium in the being there of heat and bulk diffusions. Elbashbeshy et al. [27] elaborated the effects of induction heat on free convection flow and thermal relocation over a shear cone in accordance of stressed effort and thermal source/consummation.

Bapuji et al. [28] developed a numerical form for the response of chemical process and thermal source/sink on transient streamline natural convective flow with thermal and mass transport over non-compressible viscous movement through an upright porous cone with non-homogeneous surface temperature and concentration. Sambath et al. [29] analyzed the importance of thermal emission in laminar free convective hydro magnetic movement of viscous dissipation fluid past an upright cone with mass transport under the influence of chemical reaction. A numerical solution of 3-dimensional movement over a non-linear stretch surface was presented by Mahanthesh et al. [36]. Gireesha et al. [37] reported the effects of the thermal emission and Hall effect on boundary layer flow past a variable stretching surface. Radiative non-linear three dimensional movement of ferrofluid with joule heating, convective state and coriolis force has been reported by Kumar et al. [38]. Mahanthesh et al. [39–41] presented the boundary layer two-phase movement and heat flux of Casson liquid with different aspects. Gireesha et al. [42] presented the solutions of the problem of radiation aspects in kerosene-alumina nanoliquid movement owing to heat source and variable viscosity. Makinde et al. [43] reported the effects of temperature and exponential space reliant sources on MHD-nanoliquid movement crossways a rotary disk with water based nanoliquids contain aluminum and titanium alloy nanoparticles are discussed. Having all above discussion in view, the present research work is conducted to explore the various physical effects on hydromagnetic movement of viscous fluid induced by cone.

The current investigation, namely a numeral solution is accessible for transient laminar natural convection from a vertical cone with uniform surface heat flux with MHD, heat generation/absorption, viscous dissipation and thermal radiation effects. The governed boundary layer equations are explained by an implicit finite difference scheme of Crank-Nicolson method. The graphical outcomes are shown for the velocities, thermal, local and average shear stress and Nusselt numeral profiles. The study finds important applications in industrial manufacturing processes, geophysical heat transfer and hybrid solar energy systems. According to the best knowledge of authors, no such study exists in the literature.

Mathematical Modeling

A two-dimensional free convection of thermal liquid or gas caused by molecular motion of viscous fluid over an vertical cone with homogeneous heat flux is confer into account. The effects of viscous dissipation are viewed or the sensation caused by heat energy is carefully weighed with the following assumptions.

(i) The attractive field is non-varying in a bearing vertical to the cone surface.
(ii) The induced current does not deform the magnetic field.
(iii) The co-efficient of electrically conductivity is constant and scalar all over the fluid.
(iv) The Joule heating of the liquid is neglected.
(v) The effects of pressure gradient, viscous and magnetic dissipations are negligible.
(vi) Thermal radiation is current in the form of a unidirectional flux q_r and y direction.
(vii) The radiative thermal flux in the x direction is considered small in judgment among that in the y direction.
(viii) The fluid believed is a gray absorbing/emitting, but non-distribution medium. Roseland approximation calculation is applied in the power equation for the radiative thermal flux.

The co-ordinate system is chosen such to establish position is give an exhibition of to an interested study has been consider as x-axis is taken along the surface of the cone from the vertex $x=0$ and y denotes the space taken vertical to x (see Fig. 1). The fluid belongings are taken to be unvarying and take exception to density divergence which stimulates perkiness power term in the velocity equation and it maneuver key factor the discussion. Here ϕ denote the half vertical angle of the cone and $r(x)$ is the local radius of the cone.

Primarily at $t' \leq 0$, it is considered that the cone surface and the enclosing fluid which is at rest have the same temperature T'_{∞}. Then at $t' > 0$, temperature of cone surface is suddenly raised to uniformly q_w. It is considered that the liquid property is non-varying excepting for mass variation which induces optimism power expression in the thrust equation. The leading boundary layer equation of stability, an impelling force or strength and thermodynamic quantity equivalent to the capacity of a physical system to do work which was proved by an approximation given by Boussinesq are stated below:

Equation of continuity:

$$\frac{\partial}{\partial x}(ru) + \frac{\partial}{\partial y}(rv) = 0. \tag{1}$$

Equation of momentum:

$$\frac{\partial u}{\partial t'} + u\frac{\partial u}{\partial x} + v\frac{\partial u}{\partial y} = g\beta(T' - T'_{\infty})cos\phi + \nu\frac{\partial^2 u}{\partial y^2} - \frac{\sigma B_0^2 u}{\rho}. \tag{2}$$

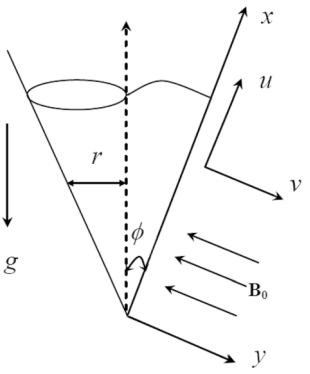

Fig. 1 Physical model and co-ordinate system

Equation of energy:

$$\frac{\partial T'}{\partial t'} + u\frac{\partial T'}{\partial x} + v\frac{\partial T'}{\partial y} = \alpha\frac{\partial^2 T'}{\partial y^2} + \frac{\mu}{\rho C_P}\left(\frac{\partial u}{\partial y}\right)^2 - \frac{1}{\rho C_P}\frac{\partial q_r}{\partial y} + \frac{Q_0}{\rho C_P}(T' - T'_\infty). \tag{3}$$

The primary and boundary conditions be

$$\left.\begin{aligned} t' \le 0 :\ u = 0,\ v = 0,\ T' = T'_\infty, \text{for all } x \text{ and } y \\ t' > 0 :\ u = 0,\ v = 0,\ \frac{\partial T'}{\partial y} = -\frac{q_w}{k^{**}} \text{ at } y = 0 \\ u = 0,\ T' = T'_\infty \text{ at } x = 0 \\ u \to 0,\ T' \to T'_\infty \text{ as } y \to \infty \end{aligned}\right\}, \tag{4}$$

$$q_r = \frac{-4\sigma^*}{3k^*}\frac{\partial T'^4}{\partial y}, \tag{5}$$

$$T'^4 \cong T'^3_\infty T' - 3T'^4_\infty, \tag{6}$$

$$\frac{\partial q_r}{\partial y} = \frac{16\sigma^* T'^3_\infty}{3k}\frac{\partial^2 T'}{\partial y^2}. \tag{7}$$

Using the Rosseland's approximation calculation for radiation, the radiative heat flux is simplify as

$$\frac{\partial T'}{\partial t'} + u\frac{\partial T'}{\partial x} + v\frac{\partial T'}{\partial y} = \alpha\frac{\partial^2 T'}{\partial y^2} + \frac{\mu}{\rho C_P}\left(\frac{\partial u}{\partial y}\right)^2 - \frac{1}{\rho C_P}\frac{16\sigma^* T'^3_\infty}{3k^*}\left(\frac{\partial^2 T'}{\partial y^2}\right) + \frac{Q_0}{\rho C_P}(T' - T'_\infty). \tag{8}$$

Further, introducing the subsequent dimensionless values:

$$\left.\begin{aligned} &X = \frac{x}{L},\ Y = \frac{y}{L}(Gr_L)^{1/5},\ R = \frac{r}{L} \text{ where } r = x\sin\phi \\ &t = \frac{\nu t'}{L^2}(Gr_L)^{1/5}, T = \frac{(T' - T'_\infty)}{q_w/k^{**}}(Gr_L)^{1/5},\ U = \frac{uL}{\nu}(Gr_L)^{-1/5}, \\ &V = \frac{vL}{\nu}(Gr_L)^{-1/5},\ Pr = \frac{\nu}{\alpha},\ Rd = \frac{k^* k}{4\sigma^* T'^3_\infty},\ \Delta = \frac{Q_0 L^2}{C_P \mu}(Gr_L)^{-1/5}, \\ &M = \frac{\sigma B_0^2 L^2}{\mu}(Gr_L)^{-1/5},\ Gr_L = \frac{g\beta(q_w/k^{**})\cos\phi}{\nu^2}, \varepsilon = \frac{g\beta L}{C_P}, \\ &\nu = \frac{\mu}{\rho} \end{aligned}\right\} \tag{9}$$

Equations (1)–(3) are written in the subsequent dimensionless form:

$$\frac{\partial}{\partial X}(UR) + \frac{\partial}{\partial Y}(VR) = 0, \tag{10}$$

$$\frac{\partial U}{\partial T} + U\frac{\partial U}{\partial X} + V\frac{\partial U}{\partial Y} = T + \frac{\partial^2 U}{\partial Y^2} - MU, \tag{11}$$

$$\frac{\partial T}{\partial t} + U\frac{\partial T}{\partial X} + V\frac{\partial T}{\partial Y} = \frac{1}{\mathrm{Pr}}\left(1 + \frac{4}{3Rd}\right)\frac{\partial^2 T}{\partial Y^2} + \Delta T + \varepsilon\left(\frac{\partial U}{\partial Y}\right)^2. \tag{12}$$

The equivalent dimensionless initial and boundary condition are

$$\left.\begin{aligned} &t \le 0 : \ U = 0,\ V = 0,\ T = 0, \text{ for all X and Y},\\ &t > 0 : \ U = 0,\ V = 0,\ \frac{\partial T}{\partial Y} = -1 \text{ at Y} = 0,\\ &U = 0,\ T = 0 \text{ at X} = 0,\\ &U \to 0,\ T \to 0 \text{ as } Y \to \infty \end{aligned}\right\}. \tag{13}$$

The substantial quantity of shear stress and heat transfer rate are given below.

$$\tau_x = \mu\left(\frac{\partial u}{\partial y}\right)_{y=0} \tag{14}$$

$$Nu_x = \frac{-x}{T'_w - T'_\infty}\left(\frac{-\partial T'}{\partial y}\right)_{y=0}. \tag{15}$$

Skin-friction and Nusselt number in dimensionless quantities is given by

$$\tau_X = (Gr_L)^{3/5}\left(\frac{\partial U}{\partial Y}\right)_{Y=0}, \tag{16}$$

$$Nu_X = \frac{X}{T_{Y=0}}\left(\frac{-\partial T}{\partial Y}\right)_{Y=0}(Gr_L)^{1/5}. \tag{17}$$

Average skin-friction and average Nusselt number in dimensionless forms are

$$\bar{\tau} = 2(Gr_L)^{3/5}\int_0^1 X\left(\frac{\partial U}{\partial Y}\right)_{Y=0} dX, \tag{18}$$

$$\overline{Nu} = 2(Gr_L)^{1/5}\int_0^1 \frac{X}{T_{Y=0}}\left(\frac{-\partial T}{\partial Y}\right)_{Y=0} dX. \tag{19}$$

Methodology

The nonlinear coupled PDE (10) to (12) with (13) are computed through Crank–Nicholson scheme. The non-dimensional equations transformed to the scheme of tri-diagonal expressions. The solution is brought out via Thomas algorithm. The convergence of this algorithm achieved at small time-period Soundalgekar and Ganesan [30], Ganesan and Rani [31] and Ganesan and Palani [32]. The integral area is treat as a square or with $X_{\max} = 1$ and $Y_{\max} = 26$. Where corresponds to Y is taken to be ∞ which lies very well outside both momentum and thermal boundary layers. We considered the order to satisfy penultimate and ultimate conditions (13). It is observed that an accuracy up to 10^{-5} is found. The meshing range has been mending as $\Delta X = 0.05,\ \Delta Y = 0.05$ taking an increment of step size being $\Delta t = 0.01$. The truncation error is $O(\Delta t^2 + \Delta Y^2 + \Delta X)$ approaches to null value as $\Delta t, \Delta Y$ and ΔX approaching the quantity of null. Based on the above calculations, computations and approximations, we come to the conclusion that an elaborate and systematic plan of action shows a solution can be able to exist and perform in harmonious as explained [29].

Results and Discussion

The division provides the behavior of different physical parameter concerned in the expressions of velocity, thermal, shear stress co-coefficient and Nusselt numeral ratio. In regulate to confirm the exactness of our arithmetic outcome, the outcome in steady position at X = 1.0 is attained. Mathematical value of Prandtl number is shown in Table 1 and the values are comparing by the results of Palani and Kim [33] in steady state. In addition, it is noticed that the near results concur fine by Pop and Watanabe [34], Na and Chiou [35].

Table 1: Relationship of steady-state shear stress values at X = 1 with those of Palani and Kim [33].

Table 1 Numerical illustrations of comparative data for different values of *Pr*

Pr	Temperature		Local skin friction	
	Palani and Kim [33]	Present values	Palani and Kim [33]	Present values
	T	T	τ_X	τ_X
0.72	1.78840	1.7796	1.22705	1.2154
	1.7864*		1.2240*	
1	1.63454	1.6263	1.08262	
	1.6329**			
2	1.36477	1.3578	0.83155	0.8235
4	1.15169	1.1463	0.63878	0.6328
6	1.04708	1.0421	0.54736	0.5423
8	0.98001	0.9754	0.49040	0.4859
10	0.93158	0.9272	0.45021	0.4460
	0.9336**			
100	0.56289	0.5604	0.18311	0.1813
	0.5738**			

Table 2 Relationship of steady-state heat transfer rate quantities of X = 1.0 with those of Hossain and Paul [13] for dissimilar values of Pr when $M = 0$ and suction is zero

Pr	Shear stress		Heat transfer rate	
	Hossain and Paul [13]	Present results	Hossain and Paul [13]	Present results
	$F_0''(0)$	$\tau_X/G_{r_L}^{3/5}$	$1/\Phi_0(0)$	$Nu_X/Gr_L^{1/5}$
0.01	5.1345	5.1155	0.14633	0.1458
	5.13424[#]		0.14648[#]	
0.05	2.93993	2.9297	0.26212	0.2630
	2.93180[#]		0.26227[#]	
0.1	2.29051	2.2838	0.33174	0.3324
	2.29044[#]		0.33648[#]	

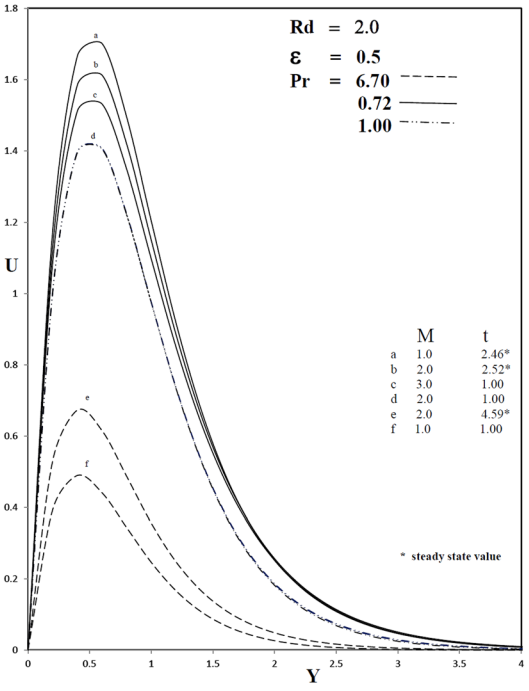

Fig. 2 Transient velocity profiles at X = 1.0 for different values of Pr and M

In Table 1 * indicates that the values obtained from Pop and Watanab [34] when suction injection is zero and ** denotes the quantities obtained from Na and Chiou [35] when solution for movement over a full cone. In addition, the shear stress co-efficient and Nusselt numeral for dissimilar values of Prandtl numeral and flux gradient at X = 1.0 in solid position are compared by Hossain and Paul [13] in Table 2. In Table 2 [#] denotes that the shear stress and heat transfer rate quantities obtained from Prakash et al. [44] for steady state purely fluid Da → ∞ case.

Figures 2 and 3 plot the variations in rate of change of displacement and thermal profile for different (Pr) and magnetic parameter (M) with heat source/absorption parameter $\Delta = 0.5$, viscous dissipation parameter $\varepsilon = 0.5$ and radiation constraint $Rd = 2.0$.

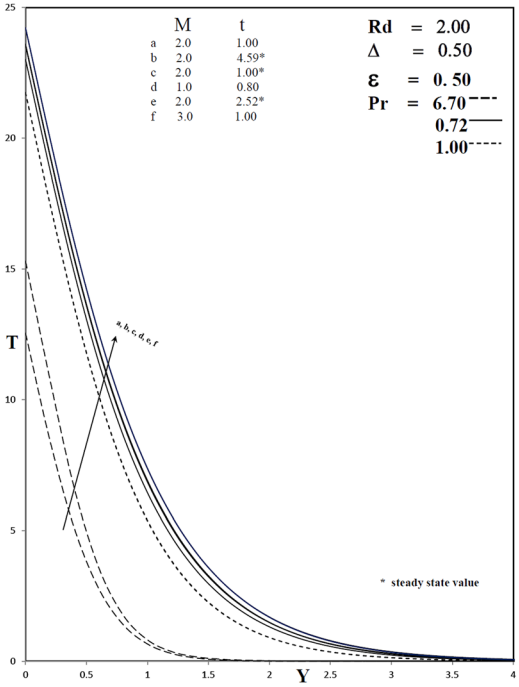

Fig. 3 Transient temperatures profiles at X = 1.0 for different values of *Pr* and *M*

It is viewed that the compatibility of an attractive ground to an electrically performing fluid draw similar power entitled the Lorentz power. This energy has the leaning to deliberate downstairs the stream along the cone surface at the outflow of expanding its temperature and a reduction in rate as *M* increases. But the trend is reversed when *Pr* increase. Figures 4 and 5 represent the velocity and thermal profile for unlike quantities of heat generation or absorption constraint Δ and radiation constraint (*Rd*) with $Pr = 0.72$, $M = 2$ and $\varepsilon = 0.5$. It shows that the rate and thermal profiles are increases with growing quantities of Δ. An increase in *Rd* from 0.5 through 1 to 3 create a major diminish in velocity among detachment into the border level. As viewed, temperature values are also notably reduced with raised in *Rd*. Figures 6 and 7 shows the behavior of velocity and temperature for varies ε when $Pr = 0.72$, $Rd = 2$, $M = 2$ and $\Delta = 0.5$. The velocity value decreases as the values of viscous dissipation increases. The temperature boundary layer thickness reduces with decreasing ε.

Figures 8 and 9 concerns the effects of *Pr* and *M* on shear stress coefficient and heat transfer rate. From these figures, it can be seen that the increasing *Pr* and *M* lead to decrease in the values of the local skin friction parameter. Also, we noted that the shear stress decrease among the decrease of the *Pr* but the trend is reversed for decreasing *M*. Figures 10 and 11 explore the effect of Δ and *Rd* on the shear stress coefficient and Nusselt number. We have seen that the larger Δ lead to a boost in the values of skin friction and reduce in the value of heat transfer rate and inverse behavior is appeared for increasing *Rd*. Figures 12 and 13 depict the effect of ε on shear stress coefficient and local Nusselt number. From these figures, it is very obvious that an increase in ε leads to increase in the values of the shear stress coefficient and decrease in the values of heat transfer rate.

The role of *Pr* and *M* on the average skin-friction and average heat transfer rate are observed in Figs. 14 and 15. A decrease in *Pr* leads to decrease in the value of the average

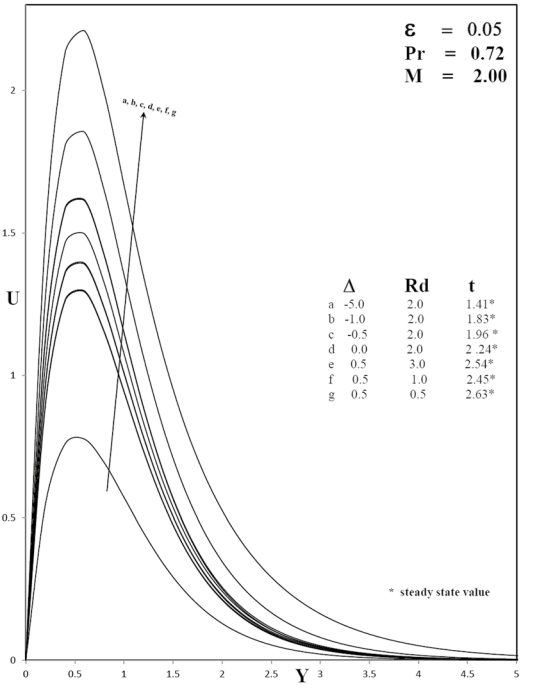

Fig. 4 Transient velocity profiles at X = 1.0 for different values of *Rd* and *Δ*

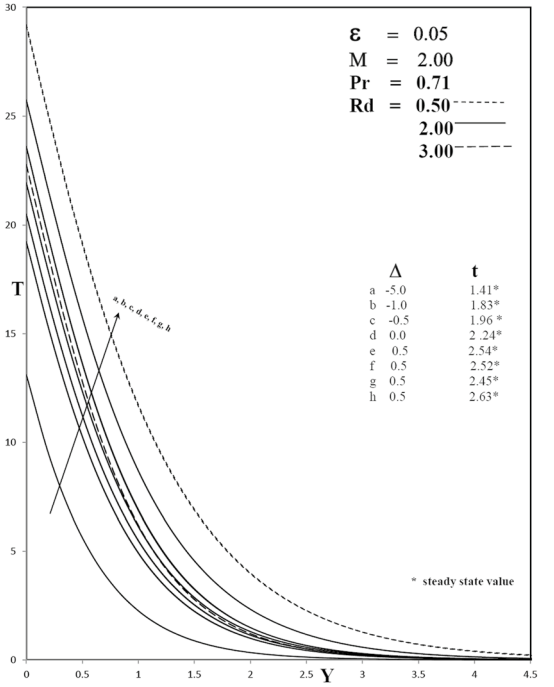

Fig. 5 Transient temperatures profiles at X = 1.0 for different values of *Rd* and *Δ*

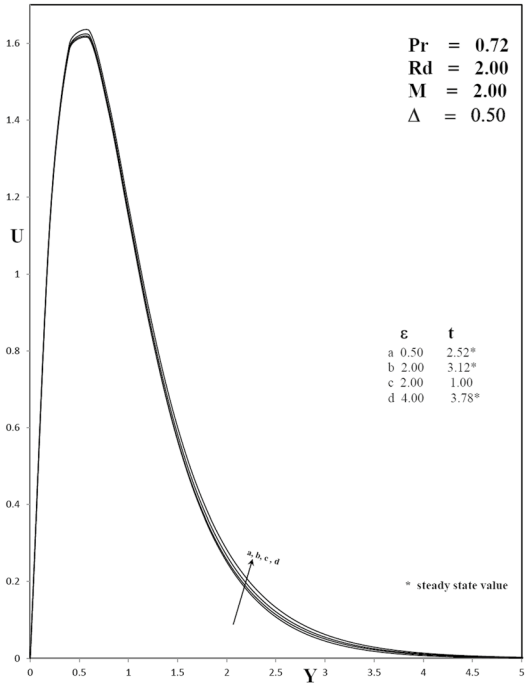

Fig. 6 Transient velocity profiles at X = 1.0 for different values of ε

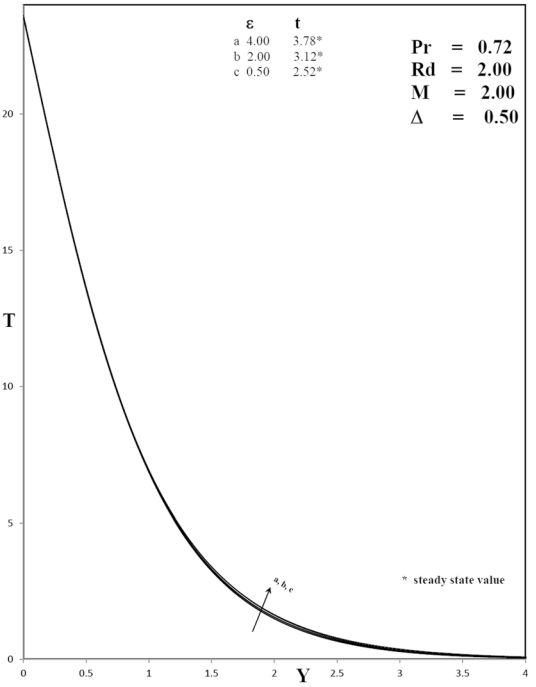

Fig. 7 Transient temperatures profiles at X = 1.0 for different values of ε

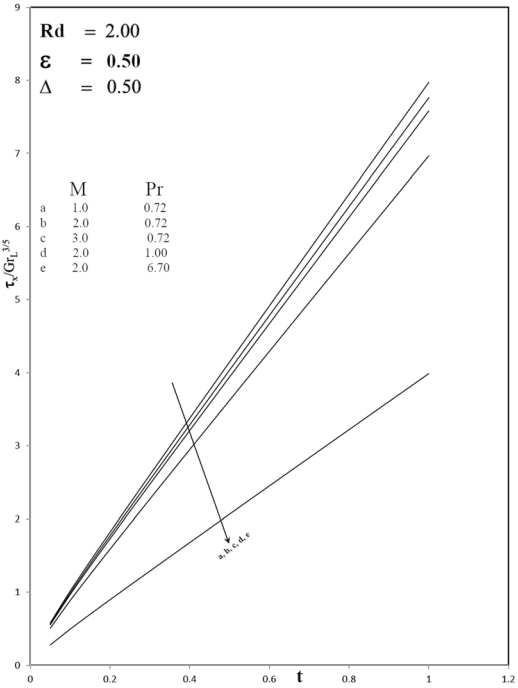

Fig. 8 Local skin friction for different values of *Pr* and *M* in transient period

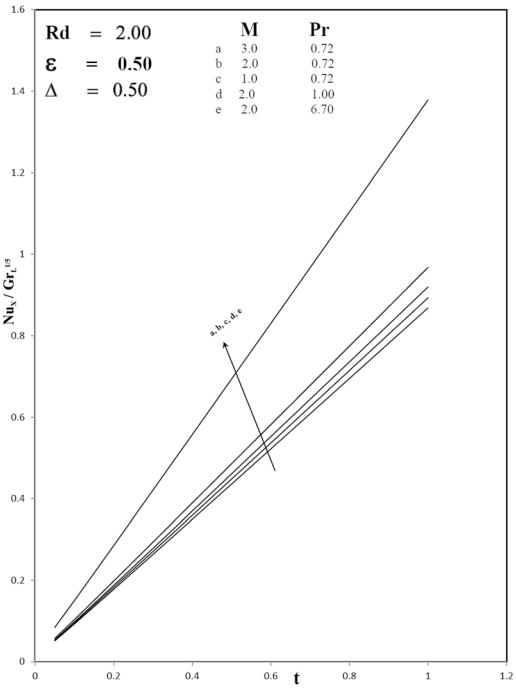

Fig. 9 Local Nusselt number for different values of *Pr* and *M* in transient period

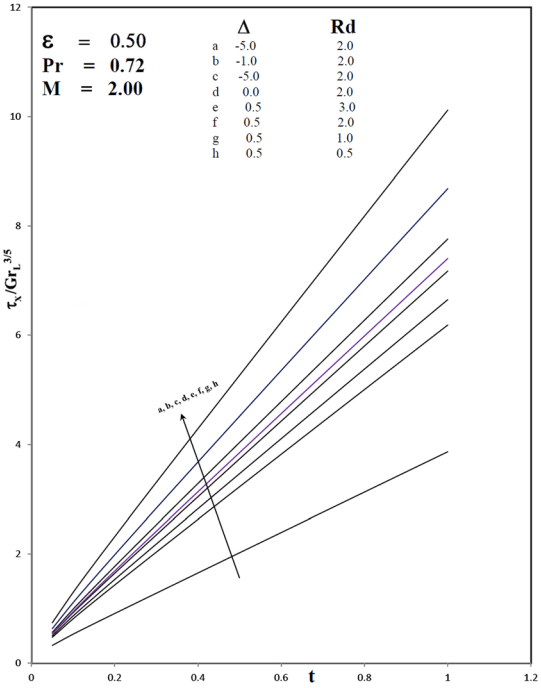

Fig. 10 Local skin friction for different values of Δ and *Rd* in transient period

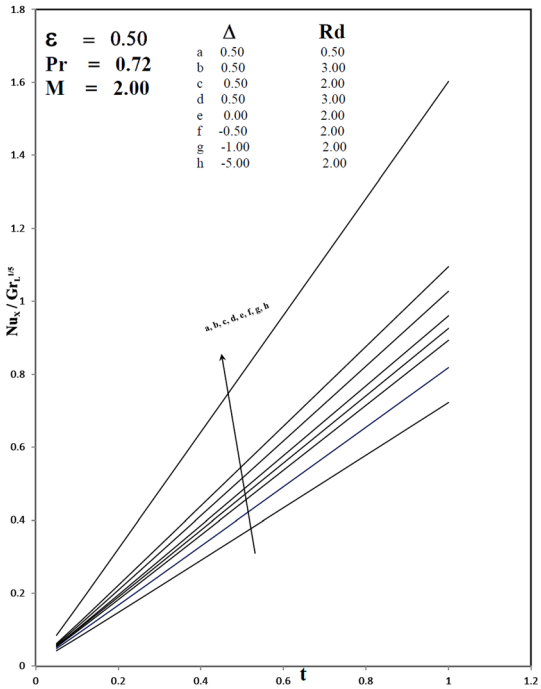

Fig. 11 Local Nusselt number for different values of Δ and Rd in transient period

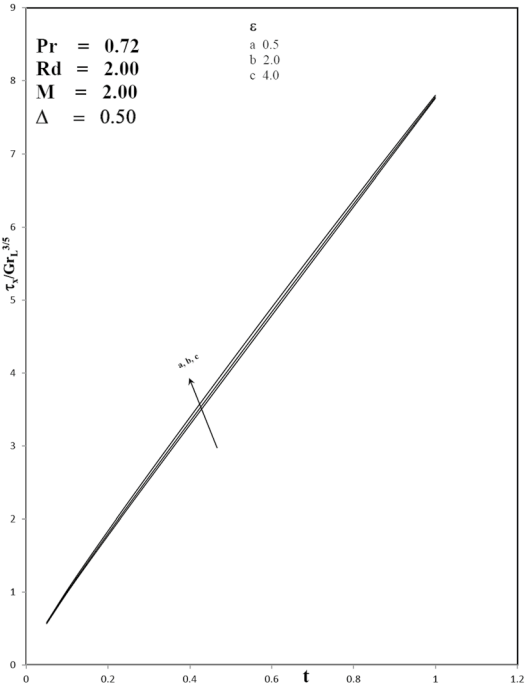

Fig. 12 Local skin friction for different values of ε in transient period

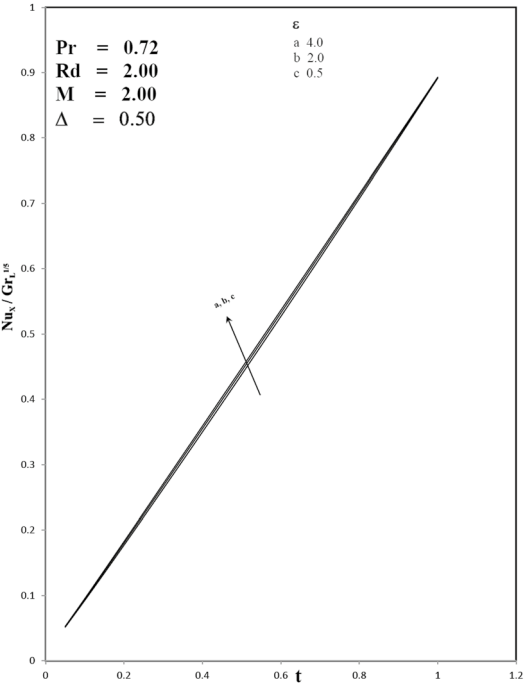

Fig. 13 Local Nusselt number for different values of ε in transient period

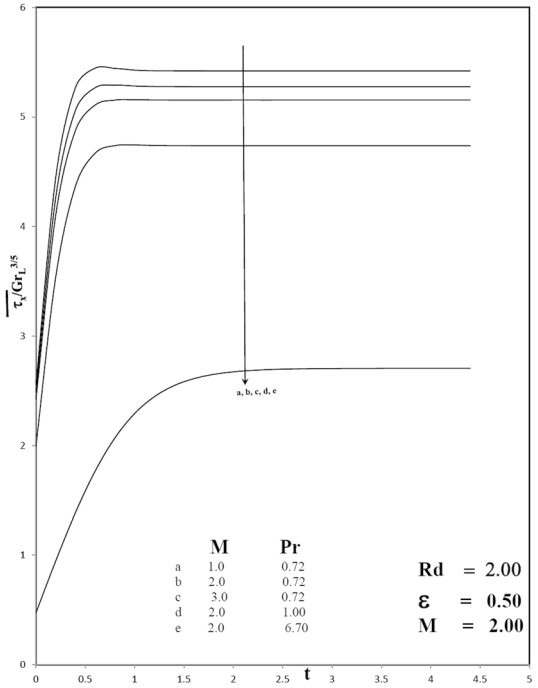

Fig. 14 Average skin friction for different values of *Pr* and *M* in transient period

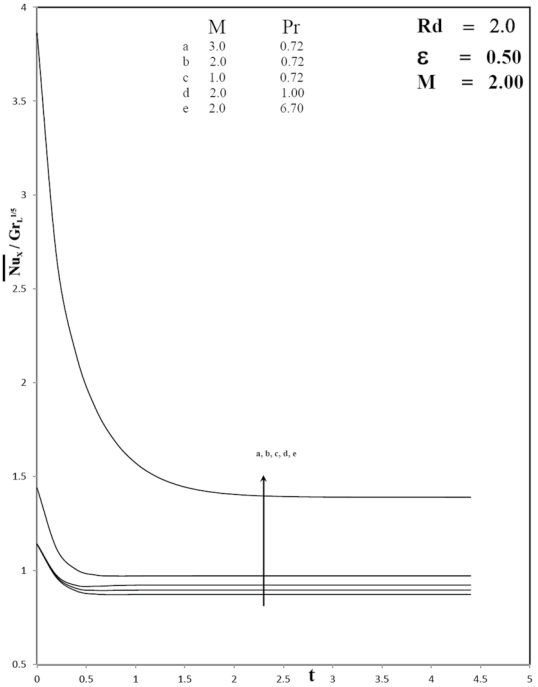

Fig. 15 Average Nusselt number for different values of *Pr* and *M* in transient period

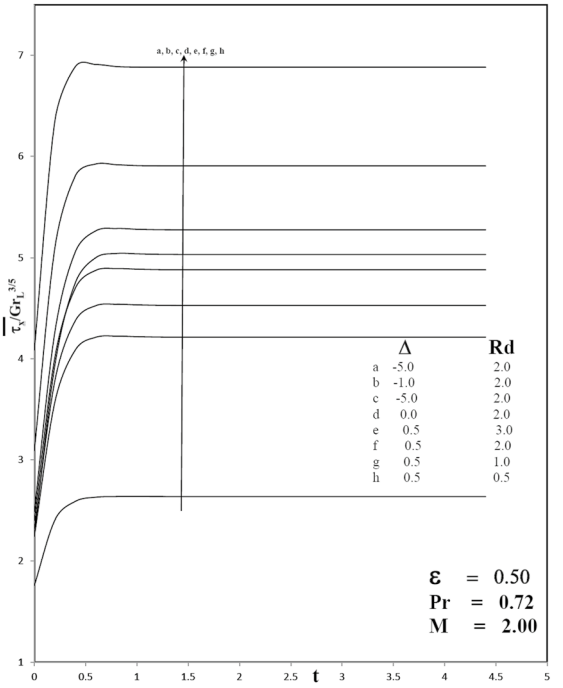

Fig. 16 Average skin friction for different values of Δ and Rd in transient period

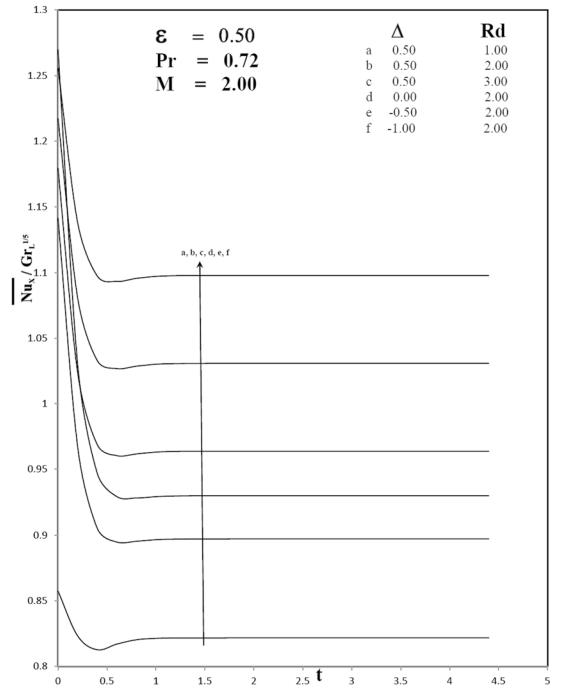

Fig. 17 Average Nusselt number for different values of Δ and Rd in transient period

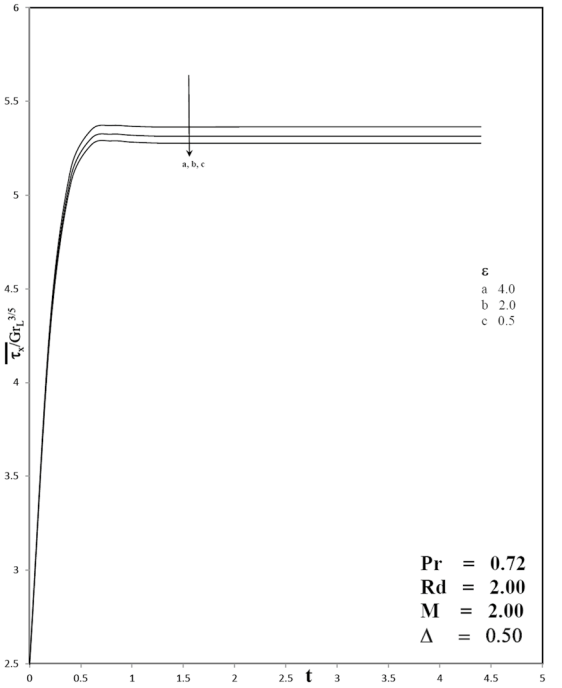

Fig. 18 Average skin friction for different values of ε in transient period

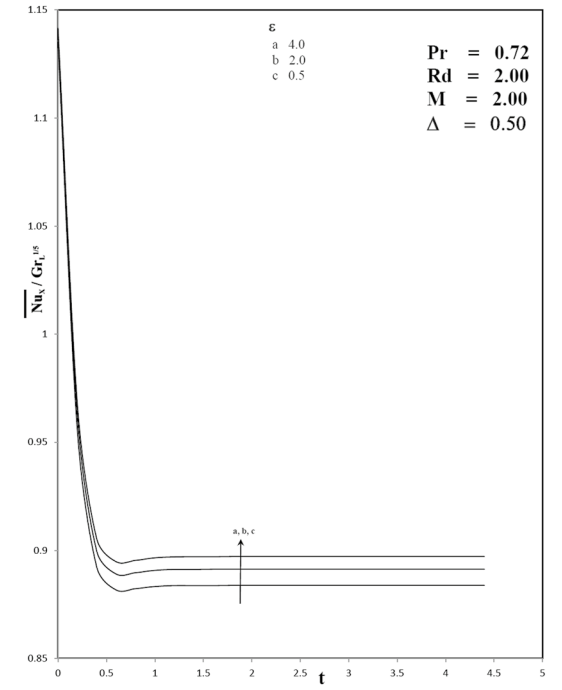

Fig. 19 Average Nusselt number for different values of ε in transient period

shear stress coefficient while M enhances the average shear stress decrease. Also, we viewed that the average heat transfer rate increase with the enhancing Pr. The trend is reversed for increasing M. Figures 16 and 17 shows the non-dimensional heat source or sink constraint Δ and radiation constraint Rd on the average shear stress and average heat transfer rate. It is observed to boost in the value of Δ lead to boost into the values of average shear stress coefficient and decrease in the value of average heat transfer rate. But the trend is reversed the radiation parameter. Figures 18 and 19 illustrate average shear stress and average Nusselt number for different viscous dissipation parameters ε. It is observed that boost in the rate of ε lead to slowly boost in the value of average shear stress coefficient and decrease slowly in the values of average heat transfer rate.

Conclusions

The present results are developed for the model of laminar convective fluid flow under the aspects of surface heat flux, magnetic field and heat absorption or generation. An electrically conducting fluid flow is generated by vertical cone. The following key features are extracted from present research.

1. The distributions of temperature and velocity decrease with the increasing values of Pr, Rd and enhance with an increment in Δ and ε.
2. An enhancement in strength of magnetic field decelerates the fluid motion along cone wall while the velocity decreases and temperature increase.
3. Shear stress coefficient τ_X and coefficient of heat transport rate Nu_X values reduces as M, Rd and Pr increase. But the trend is reversed when ε is larger.
4. An increase in the value of heat generation and heat absorption constraint Δ corresponds to increase in the value of shear stress while heat transport rate decreases.
5. The average shear stress coefficient increase for larger values of Δ, Pr, Rd, ε and lesser value of M.
6. The average heat transfer rate decreases for smaller value of Pr, Rd and higher values of M and Δ, ε.

Compliance with Ethical Standards

Conflict of interest The authors declare that they have no conflict of interest.

References

1. Gebhart, B.: Effects of viscous dissipation in natural convection. J. Fluid Mech. **14**, 225–232 (1962)
2. Alamigir, M.: Over-all heat transfer from vertical cones in laminar free convection: an approximate method. J. Heat Transf. Trans. ASME **101**, 174–176 (1979)
3. Raptis, A.: Flow through a porous medium in the presence of a magnetic field. Int. J. Energy Res. **10**, 97 (1986)
4. Lin, F.N.: Laminar free convection from a vertical cone with uniform surface heat flux. Lett. Heat Mass Transf. **3**, 49–58 (1976)

5. Chen, C.K., Chen, C.H., Minkowycz, W.J., Gill, U.S.: Non-Darcian effects on mixed convection about a vertical cylinder embedded in a saturated porous medium. Int. J. Heat Mass Transf. **35**, 3041–3046 (1992)
6. Vajravelu, K., Nayfeh, J.: Hydro magnetic convection at a cone and wedge. Int. Commun. Heat Mass Transf. **19**, 701–710 (1992)
7. Hossain, M.A., Paul, S.C.: Free convection from a vertical permeable circular cone with non-uniform surface heat flux. Heat Mass Transf. **37**, 167–173 (2001)
8. Pullepu, B., Ekambavanan, K., Chamkha, A.J.: Unsteady laminar free convection from a vertical cone with uniform surface heat flux. Nonlinear Anal. Model. Control **13**, 47–60 (2008)
9. Pullepu, B., Chamkha, A.J.: Transient laminar MHD free convective flow past a vertical cone with non-uniform surface heat flux. Nonlinear Anal. Model. Control **14**, 489–503 (2009)
10. Kumari, M., Nath, G.: Natural convection from a vertical cone in a porous medium due to the combined effects of heat and mass diffusion with non-uniform wall temperature/concentration or heat/mass flux and suction/injection. Int. J. Heat Mass Transf. **52**, 3064–3069 (2009)
11. Sunitha, S., Prasad, N.R., Reddy, B.: Radiation and mass transfer effects on MHD free convection flow past an impulsively started isothermal vertical plate with dissipation. Therm. Sci. **13**, 71–181 (2009)
12. Jordan, J.Z.: Network simulation method applied to radiation and dissipation effects on MHD unsteady free convection over vertical porous plate. Appl. Math. Model. **31**, 2019–2033 (2007)
13. Hossain, M.A., Paul, S.C.: Free convection from a vertical permeable circular cone with non-uniform surface temperature. Acta Mech. **151**, 103–114 (2001)
14. Khan, M.S., et al.: Heat generation, thermal radiation and chemical reaction effects on MHD mixed convection flow over an unsteady stretching permeable surface. Int. J. Basic Appl. Sci. **1**, 363–377 (2012)
15. Khan, M.S., et al.: Non-Newtonian MHD mixed convective power-law fluid flow over a vertical stretching sheet with thermal radiation, heat generation and chemical reaction effects. Acad. Res. Int. **3**, 80–92 (2012)
16. Mohamed, R.A., Osman, A.N.A., Abo-Dahab, S.M.: Unsteady MHD double-diffusive convection boundary layer flow past a radiative hot vertical surface in porous media in the presence of chemical reaction and heat sink. Meccanica **48**, 931 (2013)
17. Hsiao, K.: Stagnation electrical MHD nanofluid mixed convection with slip boundary on a stretching sheet. Appl. Therm. Eng. **98**, 850–861 (2016)
18. Li, J., Zheng, L., Liu, L.: MHD viscoelastic flow and heat transfer over a vertical stretching sheet with Cattaneo-Christov heat flux effects. J. Mol. Liq. **221**, 19–25 (2016)
19. Hsiao, K.: Combined electrical MHD heat transfer thermal extrusion system using Maxwell fluid with radiative and viscous dissipation effects. Appl. Therm. Eng. **112**, 1281–1288 (2017)
20. Zhao, J., Zheng, L., Zhang, X., Liu, F.: Convection heat and mass transfer of fractional MHD Maxwell fluid in a porous medium with Soret and Dufour effects. Int. J. Heat Mass Transf. **103**, 203–210 (2016)
21. Turkyilmazoglu, M.: Mixed convection flow of magnetohydrodynamic micropolar fluid due to a porous heated/cooled deformable plate: exact solutions. Int. J. Heat Mass Transf. **106**, 127–134 (2017)
22. Sheikholeslami, M., Shehzad, S.A.: Non-Darcy free convection of Fe3O4-water nanoliquid in a complex shaped enclosure under impact of uniform Lorentz force. Chin. J. Phys. **56**, 270–281 (2018)
23. Cookey, I.C., Ogulu, A., Omuho-Pepple, V.M.: The influence of viscous dissipation and radiation on unsteady MHD free convection flow past an infinite heated vertical plate in a porous medium with time dependent suction. Int. J. Heat Mass Transf. **46**, 2305–2311 (2003)
24. Chen, C.H.: MHD mixed convection of a power-law fluid past a stretching surface in the presence of thermal radiation and internal heat generation/absorption. Int. J. Nonlinear Mech. **44**, 296–603 (2008)
25. Chandrakala, P.: Radiation effects on flow past an impulsively started vertical oscillating plate with uniform heat flux. Int. J. Dyn. Fluids **6**, 209–215 (2010)
26. Seth, G.S., Hussain, S.M., Sarkar, S.: Hydro magnetic natural convection flow with heat and mass transfer of a chemically reacting and heat absorbing fluid past an accelerated moving vertical plate with ramped temperature and ramped surface concentration through a porous medium. J. Egypt. Math. Soc. **23**, 197–207 (2015)
27. Elbashbeshy, E.M.A., et al.: Effect of thermal radiation on free convection flow. Therm. Sci. **20**, 555–565 (2016)
28. Pullepu, B., Sambath, P., Viswanathan, K.K.: Effects of chemical reactions on unsteady free convective and mass transfer flow from a vertical cone with heat generation/absorption in the presence of VWT/VWC. Math. Probl. Eng. **2014**, 1–20 (2014). **(Id 849570)**
29. Sambath, P., Pullepu, B., Hussain, T., Shehzad, S.A.: Radiated chemical reaction impacts on natural convective MHD mass transfer flow induced by a vertical cone. Results Phys. **8**, 304–315 (2018)

30. Soundalgekar, V.M., Ganesan, P.: Finite difference analysis of transient free convection with mass transfer on an isothermal vertical flat plate. Int. J. Eng. Sci. **19**, 757–770 (1981)
31. Ganesan, P., Rani, H.P.: Unsteady free convection on vertical cylinder with variable hat and mass flux. Heat Mass Transf. **35**, 259–265 (1999)
32. Ganesan, P., Palani, G.: Finite difference analysis of unsteady natural convection MHD flow past an inclined plate with variable surface heat and mass flux. Int. J. Heat Mass Transf. **47**, 4449–4457 (2004)
33. Palani, G., Kim, K.Y.: Influence of magnetic field and thermal radiation by natural convection past vertical cone subjected to variable surface heat flux. Appl. Math. Mech. **33**, 605–620 (2012)
34. Pop, I., Watanabe, T.: Free convection with uniform suction or injection from vertical cone for constant wall flux. Int. Commun. Heat Mass Transf. **19**, 275–283 (1992)
35. Na, T.Y., Chiou, J.P.: Laminar natural convection over a frustum of a cone. Appl. Sci. Res. **35**, 409–421 (1979)
36. Mahanthesh, B., Gireesha, B.J., Reddy Gorla, R.S., Abbasi, F.M., Shehzad, S.A.: Numerical solutions for magnetohydrodynamic flow of nanofluid over a bidirectional non-linear stretching surface with prescribed surface heat flux boundary. J. Magn. Magn. Mater. **417**, 189–196 (2016)
37. Gireesha, B.J., Mahanthesh, B., Reddy Gorla, R.S., Manjunatha, P.T.: Thermal radiation and Hall effects on boundary layer flow past a non-isothermal stretching surface embedded in porous medium with non-uniform heat source/sink and fluid particle suspension. Heat Mass Transf. **52**(4), 897–911 (2016)
38. Sampath Kumar, P.B., Gireesha, B.J., Mahanthesh, B., Gorla, R.S.R.: Radiative non-linear 3D flow of ferrofluid with Joule heating, convective condition and coriolis force. Therm. Sci. Eng. Prog. **3**, 88–94 (2017)
39. Mahanthesh, B., Gireesha, B.J.: Scrutinization of thermal radiation, viscous dissipation and Joule heating effects on marangoni convective two-phase flow of Casson fluid with fluid particle suspension. Results Phys. **8**, 869–878 (2018)
40. Mahanthesh, B., Gireesha, B.J., Shehzad, S.A., Rauf, A., Sampath Kumar, P.B.: Nonlinear radiated MHD flow of nanofluids due to a rotating disk with irregular heat source and heat flux condition. Physica B Condens. Matter **537**, 98–104 (2018)
41. Mahanthesh, B., Gireesha, B.J., Sheikholeslami, M., Shehzad, S.A.: Nonlinear Radiative flow of Casson nanofluid a cone and wedge with magnetic dipole: mathematical model of renewable energy. J. Nanofluids **7**(6), 1089–1100 (2018)
42. Gireesha, B.J., Sambath Kumar, P.B., Mahanthesh, B., Shehzad, S.A., Abbasi, F.M.: Nonlinar gravitational and radiation aspects in nanofluid with exponential space dependent heat source and variable viscosity. Microgravity Sci. Technol. **30**(3), 257–264 (2018)
43. Makinde, O.D., Mahanthesh, B., Gireesha, B.J., Shashikumar, N.S., Monaledi, R.L., Tshehla, M.S.: MHD Nanofluid flow past a rotating disk with thermal radiation in the presence of aluminium and titanium alloy nanoparticles. Defect Diffus. **384**, 69–79 (2018)
44. Prakash, J., Gouse Mohiddin, S., Vijaya Kumar Varma, S.: Free convective MHD flow past a vertical cone with variable heat and mass flux. J. Fluids **2013**, 404985 (2013)